THE PERFORMANCE COMPUTATION OF THE HOT AIR ANTI-ICING SYSTEM OF AN AERO-ENGINE CONE

Dong Wei, Zhu Jianjun, and Cai Yinglei
Shanghai Jiao Tong University
wdong@sjtu.edu.cn;zorro2005@sjtu.edu.cn;caicaihello@163.com

Keywords: *Anti-icing, Heat transfer, Droplet impingement property, Aero-engine Cone, Water Droplet*

Abstract

Ice accretion on the inlet of an aero-engine could adversely affect the characteristics of the inlet flow field and degrade the engine's performance. When the accrued ice sheds, the ice sucked into the engine could induce serious damages. In order to reduce the hazards caused by in-flight icing, an anti-icing or de-icing system should be used. Hot air bleeding from high pressure compressor is widely used in the inlet anti-icing system, such as the cone and inlet guide vane. The anti-icing system can prevent ice accretion on the inlet component's surface, and consequently ensure the flying safety.

A numerical method of the temperature prediction on the cone surface under icing conditions is presented. The flow field of external and internal flow is solved in 2D axisymmetric coordinate by using Fluent. The droplets impingement property and surface temperature of the cone are predicted by external solver which based on the energy balance analysis. Comparisons between the computational results and the experimental data are presented.

1 Introduction

Ice accretion on the inlet of an aircraft engine usually causes degradation in the engine's performance and the shedding ice might be sucked into the engine, leading serious damages. Hot air anti-icing systems are widely used to prevent ice accretion on the inlet surface, such as the cone and inlet guide vane. The hot air anti-icing system prevents ice accretion on the cone surface by evaporating or partially evaporating super-cooled droplets which impinge on the surface. The partially evaporating anti-icing system allows the impinged liquid water run back on the surface. Most of inlet components of an aero-engine adopt wholly evaporating anti-icing system without permitting the ice accumulation on the inlet surfaces.

Certification procedures have been established to ensure the aircraft engine safe operation under all kinds of icing conditions [1, 2]. Though significant efforts have been devoted to the research of icing physics and icing protection, a successful prediction of icing accretion and the design of an anti-icing system still requires further studies and improvements. In recent years, many computational models of the icing problem were developed to improve the design of icing protection systems. Computational codes of icing have been developed at NASA(ANTICE[3], LEWICE [4,5], McGill University[6], ONERA, DAR, et al. These icing simulations consist of four basic steps[7]:computation of aerodynamic flow; determination of super-cooled water droplet trajectories and local collection efficiency; thermal balance analysis of the air-water-ice-wall; determination of the shape of the ice accretion. For the analysis of evaporating anti-icing systems, the step of icing shape prediction can be eliminated as no ice is allowed to accumulate on the surface of component. Flow field around the body can be obtained by solving Euler or Navier-Stokes equations and the convective heat transfer coefficient on the icing surface can be obtained at the same time.

Super-cooled water droplet trajectories can be tracked using a Lagrangian approach and subsequently the local collection efficiency on the surface can be calculated[8,9,10]. Another approach to determine the mass of water droplets that impinge on the surface is Eulerian approach which solves flow field and the water droplets equation of motion using the same grid and numerical techniques. Bourgault et al.[11] have developed code using Eulerian approach to calculated water impact loads on complex geometries. Both of Lagrangian approach and Eulerian approach can give satisfied water droplet impingement results. Most ice accretion codes compute the surface temperature and predict the ice growth rate using heat and mass balance model given by Messinger[12]. The heat balance model is important for predicting ice accretion process and affects the result of the ice shape. The physics behind icing problem are not well known and the models are improved continuously in order to solve this complex problem more accurately. Al-Khalil[13,14] utilizes the breakup of a uniformly thin liquid film into individual streams or rivulets to more accurately describe the physics of runback water. Yi X[15] modified the icing model and used it for numerical simulation of rime, glaze and mixed ice accretion on the airfoil surface. Silva et al.[16] developed a thermal model considering coupled and mass transfer effects for anti-icing numerical simulation. Croce G[17] computed the temperature on the icing surface by solving 3D Navier-Stokes equations and solid conduction equation. Dong W et al.[18,19] computed and analyzed the performance of a hot air anti-icing system and a hot oil anti-icing system using conjugated algorithm

A few researches paid attention to aero-engine anti-icing components, and little report focused on the droplet impingement property and temperature distribution on the cone surface of aero-engine under icing conditions. In this paper, a computational method of the temperature prediction on the cone surface under icing conditions is presented. The flow field of external and internal flow is solved in 2D axisymmetric coordinate by using Fluent. The droplets impingement property and surface temperature of the cone are predicted by external solver which based on the energy balance analysis. The effectiveness of the method is validated by comparing with the experimental data.

2 Mathematical Models

2.1 Governing Equations of Flow Field

Flow field is need before calculating the droplet impingement property and surface temperature of the cone. The flow field around the aero-engine cone can be obtained by solving the mass equation, momentum equations and energy equation using Fluent axisymmetric solver. The N-S equations of steady flow in 2D axisymmetric coordinate can be described as follows,

Mass conservation equation

$$\frac{\partial(\rho v_x)}{\partial x}+\frac{\partial(\rho v_r)}{\partial r}+\frac{\rho v_r}{r}=0 \qquad (1)$$

Axial momentum conservation equation

$$\begin{aligned}&\frac{1}{r}\frac{\partial}{\partial x}(r\rho v_x v_x)+\frac{1}{r}\frac{\partial}{\partial r}(r\rho v_r v_x)\\&=-\frac{\partial p}{\partial x}+\frac{1}{r}\frac{\partial}{\partial x}\left[r\mu\left(2\frac{\partial v_x}{\partial x}-\frac{2}{3}\nabla\cdot\vec{v}\right)\right]\\&+\frac{1}{r}\frac{\partial}{\partial r}\left[r\mu\left(\frac{\partial v_x}{\partial r}+\frac{\partial v_r}{\partial x}\right)\right]\end{aligned} \qquad (2)$$

Radial momentum conservation equation

$$\begin{aligned}&\frac{1}{r}\frac{\partial}{\partial x}(r\rho v_x v_r)+\frac{1}{r}\frac{\partial}{\partial r}(r\rho v_r v_r)\\&=-\frac{\partial p}{\partial r}+\frac{1}{r}\frac{\partial}{\partial x}\left[r\mu\left(\frac{\partial v_r}{\partial x}+\frac{\partial v_x}{\partial r}\right)\right]\\&+\frac{1}{r}\frac{\partial}{\partial r}\left[r\mu\left(2\frac{\partial v_r}{\partial r}-\frac{2}{3}\nabla\cdot\vec{v}\right)\right]\\&-2\mu\frac{v_r}{r^2}+\frac{2}{3}\frac{\mu}{r}(\nabla\cdot\vec{v})\end{aligned} \qquad (3)$$

In such a coordinate, the divergence of air velocity $\nabla\cdot\vec{v}$ can be extended as the following form,

$$\nabla \cdot \vec{v} = \frac{\partial v_x}{\partial x} + \frac{\partial v_r}{\partial r} + \frac{v_r}{r} \tag{4}$$

Energy conservation equation

$$\frac{\partial}{\partial x}(\rho v_x T) + \frac{1}{r}\frac{\partial}{\partial r}(r\rho v_r T) = \frac{\partial}{\partial x}\left(\frac{\lambda}{c_p}\frac{\partial T}{\partial x}\right) + \frac{1}{r}\frac{\partial}{\partial r}\left(r\frac{\lambda}{c_p}\frac{\partial T}{\partial r}\right) \tag{5}$$

Where the subscripts x and r refer to the axial and radial direction respectively, and ρ, μ, λ, and c_p are density, dynamic viscosity, thermal conductivity and specific heat at constant pressure of the air respectively. v is the velocity of the air. p is the pressure of the air. T is the temperature of the air.

2.2 Droplet Impingement Property

The droplet impingement property is calculated by Lagrangian approach, which is based on the analysis of the forces on the droplet. According to Newton's second Law, the equation of motion of a droplet can be written as,

$$m_w \frac{d\vec{v}_w}{dt} = \vec{D} + \vec{G}_w \tag{6}$$

where $\vec{D}$ is the aerodynamic drag force and $\vec{G}_w$ is the droplet's gravity. $m_w, \vec{v}_w, \frac{d\vec{v}_w}{dt}$ are the mass, velocity and acceleration of the droplet respectively. As water droplets are usually very small, the droplet gravity is neglected in most cases. The drag force, $\vec{D}$,can be calculated by,

$$\vec{D} = C_D \cdot \frac{1}{2}\rho |\vec{v} - \vec{v}_w|^2 \cdot A_w \tag{7}$$

In which A_w is the frontal area facing the upstream of the droplet. The drag coefficient C_D can be computed by experience equation as follows,

$$C_D = \frac{24}{\mathrm{Re}_{rel}} \cdot (1 + 0.197\,\mathrm{Re}_{rel}^{0.63} + 2.6\times10^{-4}\,\mathrm{Re}_{rel}^{1.38}) \tag{8}$$

in which Re_{rel} is the relative Reynolds number based on the relative velocity and is given by,

$$\mathrm{Re}_{rel} = \frac{\rho_a d(\vec{v}_a - \vec{v}_w)}{\mu_a} \tag{9}$$

The subscripts a and w refer to the air and the water droplet respectively. d is the diameter of the droplet.

Local collection coefficient, β is the mass ratio of the droplets which actually impinge on the local surface and probably impinge on surface, and β can be calculated by,

$$\beta = \frac{dy \cdot r_o}{ds \cdot r_t} \tag{20}$$

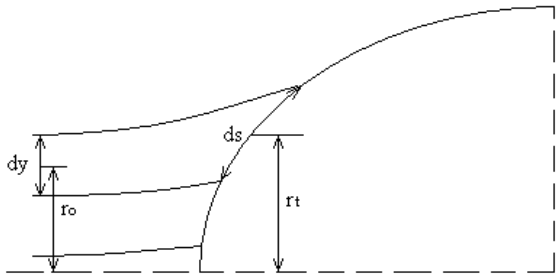

Fig.1. Definition of Local Collection Efficiency

2.3 Energy Balance on the Anti-icing Surface

When the droplets impinge on the surface of the cone, the heat flux on the surface includes convective heat transfer, sensible heating of the super-cooled water impinged on the surface, and evaporation heat transfer. The energy balance on the anti-icing surface of the cone is,

$$Q_{dropin} + Q_{antiice} = Q_{evap} + Q_{wall-air} + Q_{droph} \tag{31}$$

The left hand terms of the equation above are the heat flux of the kinetic energy contribution of the impinging droplets and internal hot air heating; while the right hand terms are the heat loss by droplets' evaporations, convective heat transfer and the increase of water enthalpy respectively.

2.4 Computation of Surface Temperature

A simplified method to predict the surface temperature distribution on the surface of the

cone under anti-icing conditions is presented in this paper,.

The temperature distribution of the cone without super-cooled water droplets impingement is computed by using conjugated computation. The energy equations of the air around cone and hot air inside the cone and the energy equation of the solid zone are solved simultaneously in a fully implicit scheme.

The local collection efficiency distribution can be calculated by Eqn.10 after trajectories of the super-cooled water droplets are computed. The impinging mass of the droplets can be obtained by,

$$\dot{m}_{imp} = \beta \cdot LWC \cdot |\vec{v}_{\infty}| \qquad (42)$$

in which LWC is the liquid water content in the air and $\vec{v}_{\infty}$ is the velocity of free stream.

Based on the results obtained by the two steps above, the heat loss caused by droplets impingement can be solved as follows,

$$\begin{aligned} Q_{ext} &= Q_{evap} + Q_{droph} - Q_{dropin} \\ &= \dot{m}_{evap} i + \dot{m}_{imp}[c_{p,d}(T_w - T_{\infty}) - \frac{v_{\infty}^2}{2}] \end{aligned} \qquad (53)$$

where i is the latent heat of water. The mass rate of water evaporated on the surface of the cone can be solved by the experience correlation,

$$\dot{m}_{evap} = \frac{0.622 I h_{air}}{c_{p,air}} \left(\frac{p_{v,water} - p_{v,e}}{p_e - p_{v,water}}\right) \qquad (64)$$

where $p_{v,water}$ and $p_{v,e}$ refers to the saturated vapor pressure at the water film temperature and the edge temperature of boundary layer respectively, which are both functions of temperature. p_e is the edge pressure of boundary layer. I is 1.1 for laminar flow while 1.0 for turbulence flow.

The surface temperature drop can be calculated as

$$\Delta T_{wall} = \frac{Q_{ext}}{\rho_{wall} c_{p,wall} d_{wall}} \qquad (75)$$

where the subscript *wall* refers to the wall of the cone. And d is the thickness of the wall of the cone.

3 Experimental Condition and Parameters

An anti-icing experiment of the cone is chosen to validate the accuracy of the numerical method presented above. The experiment was done in an icing tunnel, the experimental icing tunnel schematic is shown in Fig. 2.

The fan maintains a steady air flow in the icing tunnel, and the air is cooled down by the cooling system to meet the required temperature of the experiment condition. Water droplets are produced by the nozzles on the sprayer-bar upstream of the wind tunnel. The water droplets temperature will decrease to the temperature of the air and the velocity of water droplets will accelerate to the speed of the air after injected from nozzles.

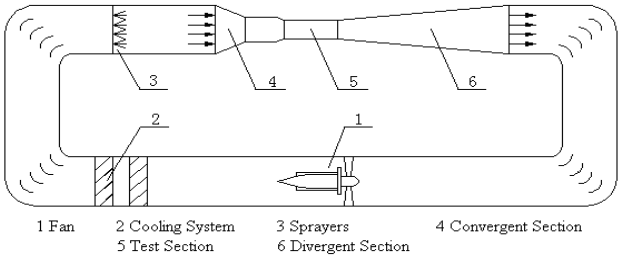

Fig.2. Schematic of the Icing Tunnel

The experimental model is a full-scale cone of an aero-engine, which is heated by the hot air produced by an electrical heater, as shown in Fig. 3. The temperature of the hot air is maintained by a PLC control system. The surface temperature distributions on the cone are measured by the thermocouples. Experimental parameters are shown in table 1.

Fig.3. Electrical Heater of Air

Table 1 Experimental Parameters

Experimental parameters	Value
Upstream temperature (K)	258
Upstream velocity (m/s)	90
Liquid water content (g/m^3)	1
MVD of water droplets (μm)	20
Hot air temperature (K)	398
Flow rate of hot air (g/s)	9.0,4.0

4 Results and Discussion

4.1 Computational Grid

The structure of the cone and the grid used in the simulation is shown in Fig.4. There are almost 60000 total cells including 3018 solid cells. Boundary layer grid is applied. The k-ω turbulence model with standard wall functions is used to simulate the turbulence flow.

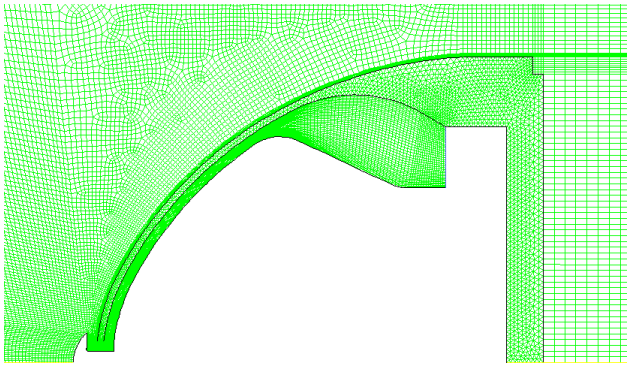

Fig.4. Computational Grid

4.2 Pressure and Velocity Distribution of the Flow Field

The pressure distribution of external flow and internal flow of the cone is shown in Fig.5. The hot air flow out from a slot and form a layer of hot air film at the leading edge of the cone. The hot air film locates at the maximum impingement region of water droplets and can effectively prevent the accumulation of ice on the leading edge of the cone. The vortex flow can be seen near the outlet of hot air from the velocity vector results shown in Fig.6.

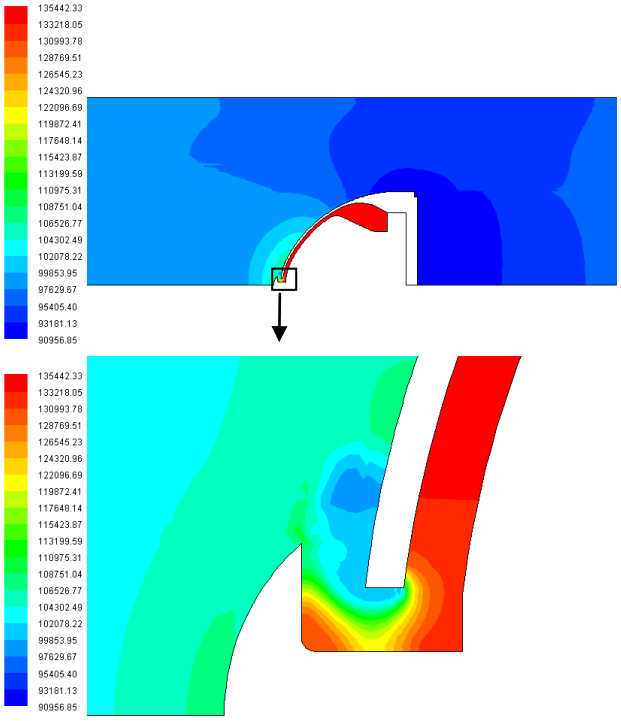

Fig. 5. Pressure Contours of external flow and internal flow of the cone when $\dot{m}_{hot}$ = 9g/s

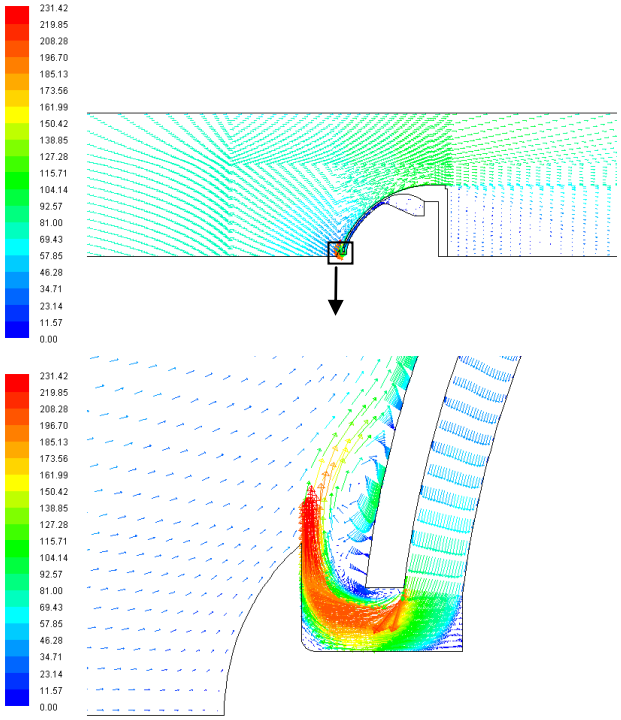

Fig.6. Velocity Vectors when $\dot{m}_{hot}$ = 9g/s

4.3 Impingement Property of Water Droplet

Impingement property of super-cooled water droplets is calculated using Lagrangian approach. Droplet trajectories shown in Fig.7

are calculated using Eqn.6. The local collection coefficient distribution on the surface of the cone is shown in Fig.8, in which the x-axis is the relative x-coordinate, $(x-x_{min})/(x_{max}-x_{min})$. It can be observed that the local collection coefficient decreases along the flow direction on the outside surface of the cone. The leading edge of the cone is the region of the largest local collection coefficient and the most easy-to-ice.

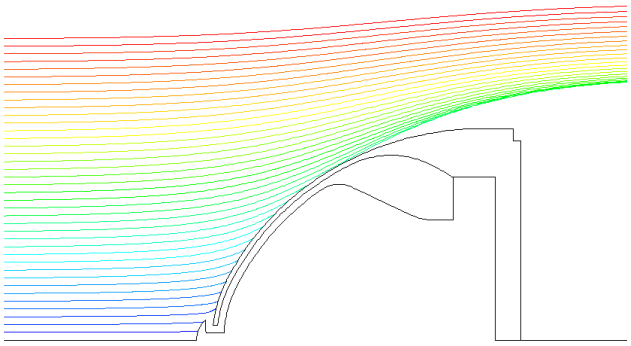

Fig. 7. Droplets Trajectories

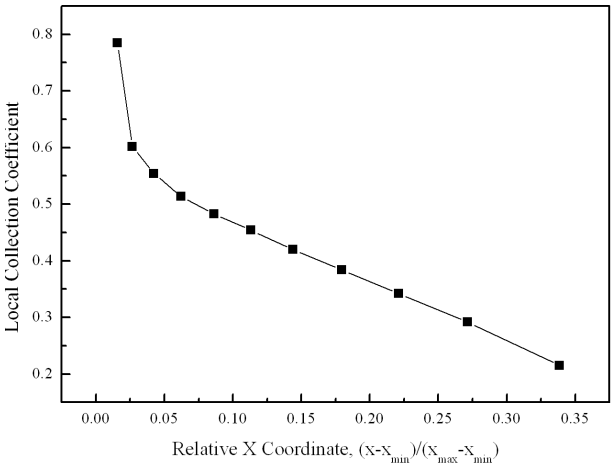

Fig.8. Local Collection Coefficient on the Cone Surface

4.4 Surface Temperature Distribution

The computational results and experimental data of the surface temperature of the cone under icing conditions are shown in Fig.9 and Fig.10. The trend of the calculated curve fits the experimental result well, which means the method presented in this paper is effective. The error between experiment and numerical simulation at the first measured point (relative x coordinate near 0.05) is much larger than others. The error is mainly due to the temperature computation without water impingement using CFD at the vortex flow region of leading edge of the cone.

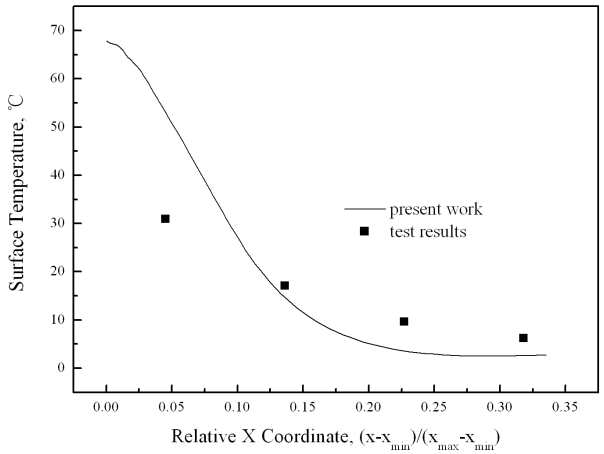

Fig.9. Surface Temperature under Icing Condition when $\dot{m}_{hot}$= 9g/s

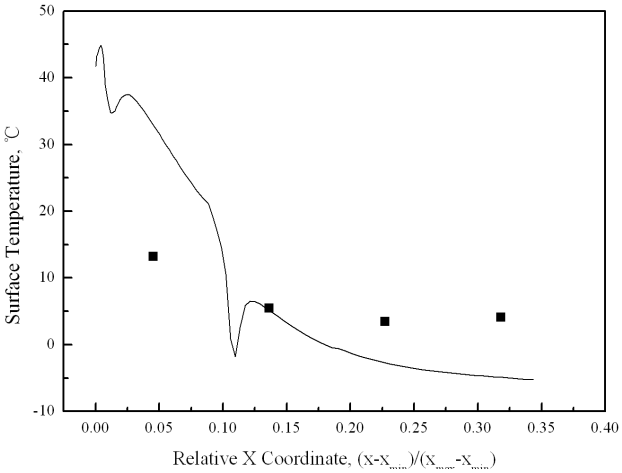

Fig.10. Surface Temperature under Icing Condition when $\dot{m}_{hot}$= 4g/s

5 Conclusion

A computational method of the temperature prediction on the cone surface under icing conditions is presented. The flow field of external and internal flow is solved in 2D axisymmetric coordinate by using Fluent. The droplets impingement property and surface temperature of the cone are predicted by external solver which based on the energy balance analysis. The effectiveness of the method is validated by comparing with the experimental data. The computational results are not satisfied at the region of the leading edge of the cone due to the complex interference flow of hot air and upstream. Further researches

should be done to improve the flow field and temperature computation by CFD and then the accuracy of the results at complex flow region using the method presented in this paper could be improved.

References

[1] Code of Federal Regulations, Title 14, Aeronautics and Space, Chapter I, Federal Aviation Administration, Part 33, Airworthiness Standards, Aircraft Engines, Section 68 - Induction System Icing and Section 77 - Foreign Object Ingestion.

[2] Code of Federal Regulations, Title 14, Aeronautics and Space, Chapter I, Federal Aviation Administration, Part 25, Airworthiness Standards: Transport Category Airplanes, Appendix C.

[3] AI-Khalil, K.M., Miller, D. and Wright, W.B., "Validation of NASA Thermal Ice Protection Computer Codes: Part 3 - Thermal Anti-Icing," AIAA-97-0051, 1997.

[4] Wright,W.B., "LEWICE 2.2 Capabilities and Thermal Validation," AIAA-2002-0383, 2002.

[5] Ghenai,C. and Lin C.X., "Verification and Validation of NASA LEWICE 2.2 Icing Software Code," *Journal of Aircraft*, Vol.43, No.5, pp.1253–1258, 2006.

[6] Pellissier, M. P. C., Habashi, W. G., and Pueyo,A., "Optimization via FENSAP-ICE of Aircraft Hot-Air Anti-Icing Systems", *Journal of Aircraft*, Vol.48, No.1, pp.265–276, 2011.

[7] Kind, R. J., Potapczuk, M. G., Feo, A., Golia, C., Shah, A. D., "Experimental and Computational Simulation of In-flight Icing Phenomena," *Progress in Aerospace Science*, Vol.34, No.5-6, pp. 257-345, 1998.

[8] Potapczuk, M. G., "A Review of NASA Lewis' Development Plans for Computational Simulation of Aircraft Icing," AIAA 99-0243, 1999.

[9] Tran, P., Brahimi, M. T., Tezok, F., Paraschivoiu, I., "Numerical Simulation of Ice Accretion on Multiple Element Configurations," AIAA 96-0869, 1996.

[10] Hou, Y. Z., "Mechanism Study on Heat Transfer and Flow of Hot Air Anti-icing for Guide Vane," M.S. Dissertation, school of Mechanical Engineering, Shanghai Jiaotong Univ., Shanghai, 2009.

[11] Bourgault, Y., Habashi, W. G., Dompierre, J., Boutanios, Z., Di Bartolomeo, W., "An Eulerian Approach to Supercooled Droplets Impingement Calculations," AIAA 97-0176, 1997.

[12] Messinger, B. L., "Equilibrium Temperature of an Unheated Icing Surface as a Function of Air Speed," *Journal of the Aeronautical Sciences*, Vol.20, pp.29–42.1953.

[13] Al-Khalil K M, Numerical Simulation of an Aircraft Anti-icing System Incorporating a Rivulet Model for the Runback Water," Ph.D. Dissertation, Univ. of Toledo, Toledo, OH, 1991.

[14] Al-Khalil, K. M., Keith, T. G., DeWitt, K. J., Nathman, J. K., Dietrich, D. A., "Thermal Analysis of Engine Anti-icing Systems," *Journal of Propulsion and Power*. Vol.6,No.5, pp.628-634, 1990.

[15] Yi, X., "Numerical Computation of Aircraft Icing and Study on Icing Test Scaling Law," Ph.D. Dissertation, China Aerodynamics Research and Development Center, Mianyang, 2007.

[16] Silva, G. A. L., Mattos Silvares, O., Jesus Zerbini, E. J. G., "Numerical Simulation of Airfoil Thermal Anti-Ice Operation Part 1: Mathematical Modeling," *Journal of Aircraft*. Vol.44, No.2, pp.627-633, 2007.

[17] Croce, G., Beaugendre, H., Habashi, W. G., "CHT3D: FENSAPICE Conjugate Heat Transfer Computations with Droplet Impingement and Runback Effects," AIAA 2002-0386, 2002.

[18] Dong, W., Zhu, J. J. and Zhao Q. Y., "Numerical Simulation Analysis of a Guide Vane Hot Air Anti-icing System", AIAA 2011-3944, 2011.

[19] Dong, W., Zhu, J., Zhou Zhixiang, Chi X., "Heat Transfer and Temperature Analysis of an Anti-icing System for an Aero-engine Strut under Icing Condition", AIAA 2012-2753, 2012.

Copyright Statement

Acknowledgement

The authors would like to recognize people who made this research program possible. The authors at Shanghai Jiaotong University were supported by the National Natural Science Foundation of China under Grant No. 51076103.